Simplifying a complex computer model: Sensitivity analysis and metamodelling of an 3D individual-based crop-weed canopy model

Floriane Colas, Jean-Pierre Gauchi, Jean Villerd, Nathalie Colbach

Simplifying a complex computer model: sensitivity analysis and metamodelling of an 3D individual-based crop-weed canopy model

Floriane Colas[1], Jean-Pierre Gauchi[2], Jean Villerd[13], Nathalie Colbach[1]

Corresponding author: nathalie.colbach@inrae.fr

[1] Agroécologie, AgroSup Dijon, INRAE, Univ. Bourgogne, Univ. Bourgogne Franche-Comté, F-21000 Dijon, France

[2] MaIAGE, INRAE, Université Paris-Saclay, 78350, France

[3] LAE, INRAE, Univ. Lorraine, F-54500 Vandœuvre-lès-Nancy, France

* Corresponding author, address:
Nathalie Colbach
UMR Agroécologie
INRAE
17 rue Sully
BP 86510
21065 Dijon Cedex
Nathalie.Colbach@inrae.fr
Tel +33-380693033
Fax +33-380693262

Declarations of interest: none

Abstract

Complex biological models such as mechanistic research models often need to extend their current use to a broader audience. Simplification and faster simulations would increase their use. Here, a step-by-step methodology was developed and applied to partially metamodel, hence accelerate, the mechanistic model FLORSYS. This is a process-based, multiannual and multispecies model ("virtual field") which simulates crop growth and weed dynamics and allows users to assess cropping systems for crop production and biodiversity. The model is relatively slow, which makes it difficult to test numerous and diverse cropping systems needed to identify those reconciling crop production and biodiversity. Here, we (1) identified the slowest submodel of FLORSYS, i.e. the 3D voxelized light interception submodel, (2) identified and applied a relevant methodology to metamodel this submodel in the simplest situation, i.e. we predicted light interception and absorption directly at the scale of the plant instead of the voxel for a single plant in a field, and (3) extrapolated the method to more complex situations, *i.e.* a plant in diverse and heterogeneous crop:weed canopies, (4) replaced the original process-based FLORSYS submodel by the metamodels, which required additional equations and decision rules, (5) evaluated the metamodelled FLORSYS with independent field observations, showing

an adequate prediction quality combined with an increased speed at fine-grained scale since the metamodelled version was 28 times faster than the process-based version. For steps 2 and 3, we used the global sensitivity method based on a truncated Legendre polynomial chaos expansion (PCE) whose coefficients were estimated by Partial Least Squares (PLS) regression to simultaneously (i) rank inputs with respect to their polynomial and total effects on outputs via the so-called PCE-PLS sensitivity indices, and (ii) provide metamodels predicting light interception and absorption at the plant level. These metamodels were then shortened into parsimonious metamodels via a LASSO-PLS method. The study showed that there was a trade-off between speed gain due to the metamodelled 3D light submodel and the speed loss due to the additional functions for neighbourhood effects. The metamodelled version is best used for testing complex systems where plant location must be modelled precisley (e.g., precision agriculture, intercropping with precision sowing) whereas the voxelized version with a large voxel size is better for simpler cropping systems. The present step-by-step process may be helpful for investigating and speeding up other complex simulation models with interacting objects/agents. It notably uses a hybrid approach, using a process-based (albeit simplified) approach for the most sensitive plant stage (newly emerged tiny plants) and separate sampling plans and metamodels to ensure that the more sensitive stages/components are adequately covered (small plants).

Keywords

Metamodel; light interception; photosynthetically active radiation PAR; crop:weed canopy; sensitivity analysis; simulation time

1 Introduction

The study of biological problems usually requires complex mechanistic models, especially when dealing with weed dynamics (Holst et al., 2007a; Colbach, 2010). Indeed, even though weeds are considered to be the most harmful pest for crop production (Oerke, 2006), national and European policies now increasingly focus on the role of weeds for biodiversity (Marshall et al., 2003; Petit et al., 2011) and the need to reduce herbicide use because of health issues and environmental concerns (Stoate et al., 2009; Waggoner et al., 2013). Unfortunately, to date, no alternative weed control technique is, alone, as efficient as herbicides, and thus, several cultural techniques must be combined to control weeds (Liebman and Gallandt, 1997). Many weed dynamics models exist to understand and predict weed dynamics (see reviews by Colbach and Debaeke, 1998; Holst et al., 2007b; Freckleton and Stephens, 2009; Bagavathiannan et al., 2020). Only a few take into account the long-term effects of the weed impacts on crops, the multiplicity of weed species, the complexity of cropping systems, or the impact on crop production and biodiversity. To date, FLORSYS (Gardarin et al., 2012; Munier-Jolain et al., 2013; Colbach et al., 2014; Colbach et al., 2021) is the one model that answers all these requirements. This is a process-based "virtual field" model which simulates the effects of cropping systems on weed dynamics as well as on crop production and weed-related biodiversity, thus making

possible a multiobjective design of cropping (Colbach et al., 2017; Colbach et al., 2021). Unfortunately, models like FLORSYS that are accurate enough to reproduce the effects of agricultural practices on weed dynamics are time-consuming and complex (Colbach, 2010). In order to use FLORSYS to screen numerous cropping systems and identify sustainable herbicide-sparse cropping systems, the model must be accelerated and simplified. This question is common to many other mechanistic models whose use is often limited by their complexity and slowness.

Complex mechanistic models can be simplified by decreasing their precision level as some problems do not require the same high precision level (Kleijnen and Sargent, 2000; Renton, 2011). To simplify a model without losing precision is more difficult and requires different methods. Global sensitivity analyses can explore the model and understand its behaviour to identify which inputs change the outputs the most. This allows developers to assign constant values to minor inputs and to simplify equations (Cox et al., 2006). Global sensitivity analyses thus help to find the correct level of complexity for a metamodel by identifying the non-influential inputs (Faivre et al., 2013). Then, metamodelling aims at emulating the original model, linking inputs and outputs by less detailed but faster equations, which simplifies model use for practical applications. Examples are metamodelling of the noTG forest model (Marie and Simioni, 2014), phoma stem canker control (Hossard et al., 2015) and the bio-geo-chemical DNDC-EUROPE model (Villa-Vialaneix et al., 2012). Sometimes, metamodelling a whole model can be impractical, particularly if there are too many inputs and outputs. If a model consists of several submodels, as is the case of FLORSYS, a more practical solution is to perform a local metamodelling on the submodel using most of the computing time (Marie and Simioni, 2014).

Metamodelling requires several steps (Kleijnen and Sargent, 2000) that summarize as (1) what is the purpose of the metamodel (*i.e.* what goal, what is the accuracy needed), (2) what do we know about the model to be metamodelled (*i.e.* which inputs, which domain of applicability, which outputs), (3) what method to use (which type of metamodel to use, which experimental design) and (4) how to evaluate the metamodel (*i.e.* what fitting, which validity). Many sensitivity analysis and metamodelling methods exist like the widespread Sobol indices or FAST. Mahévas and Iooss (2013) identified three criteria to select the best sensitivity analysis for a complex model: (1) the number of possible simulation runs, (2) the number and (3) type of inputs. The feasible number of runs, depending on the simulation time and the number of inputs are crucial to select the relevant methods (**Table 1**). When little is known about the model behaviour, which is often the case for complex models, performing early tests to increase the knowledge of the model is needed.

The objective of the present paper was to accelerate and simplify a mechanistic model, by implementing efficient metamodels through: (1) identification of the sensitivity analysis and metamodelling methods adapted to a slow, complex model such as FLORSYS, (2) identification of the

114 important inputs, (3) simplification of the equations and reduction of the computing time. We
115 voluntarily excluded technical solutions such as parallel processing or Graphical Processing Unit. We
116 focused here on the reasoning for choosing the sensitivity and metamodelling methods and how they
117 were combined with the other steps needed to transform a metamodel into a simulation model. The
118 chosen method was fully developed in Gauchi *et al.* (2017) for a preliminary study. This global
119 sensitivity analysis method is able to deal with both dependent and independent inputs. It is based on a
120 truncated Legendre polynomial chaos expansion (PCE) whose coefficients are estimated by Partial
121 Least Squares (PLS) regression (Gauchi et al., 2017) aiming to simultaneously rank inputs as a
122 function of their polynomial and total effects on outputs via the so-called PCE-PLS sensitivity indices,
123 and to provide precise and fast metamodels. Finally, the metamodels were reduced into parsimonious
124 metamodels via a LASSO-PLS regression method.

125 The methodology to accelerate and simplify FLORSYS involves several steps (Figure 1). Section 2
126 presents the target model and its submodels in order to identify the most time-consuming submodel
127 (i.e., the light-interception submodel, step 1). Section 3 first presents the metamodelling approach *per*
128 *se*, with the tests that led to the choice of the most suitable method working with a simple case study
129 (*i.e.* a single plant in the field, step 2), and then how we applied this method to cover all situations in
130 the model (i.e., target plants surrounded by neighbour plants, step 3). Finally, section 4 demonstrates
131 how the metamodels were integrated into FLORSYS (step 4), and section 5 uses field observations to
132 investigate which model (process-based vs metamodel) is the best in terms of simulation speed and
133 precision, depending on the model use (step 5).

134 2 Identification of the model constraints

135 2.1 Presentation of FLORSYS

136 FLORSYS (Gardarin et al., 2012; Munier-Jolain et al., 2013; Colbach et al., 2014; Colbach et al., 2021)
137 is a mechanistic (*i.e.* process-based) model which simulates multispecies weed dynamics depending on
138 the cropping system and pedoclimate in a "virtual field". Its purpose is to experiment numerous
139 cropping systems to design sustainable weed management strategies that reconcile reduced herbicide
140 use, crop production and biodiversity. FLORSYS simulates the annual life-cycle of crop and weed
141 plants at a daily time step and is a combination of submodels such as plant emergence, plant growth or
142 radiation interception. FLORSYS inputs are daily weather, soil characteristics, initial weed seed bank,
143 and cropping system practices (crop succession and detailed list of cultural operations). Outputs
144 include crop yield, daily weed seed bank, plant densities and biomass (for more information see
145 supplementary materiel online S1). As FLORSYS consists of a collection of submodels, the
146 simplification should not concern the whole model, but individual submodels should be simplified
147 individually to keep modularity and access to specific submodels outputs.

2.2 Identification of the most time-consuming submodel in FLORSYS (step 1)

The computing time for each FLORSYS submodel was registered for a simulation with diverse crops and cultural practices over 13 years corresponding to a cropping system trial (Colbach et al., 2016a). Code profiling of the C++ source code of FLORSYS showed that the 3D radiation interception submodel was by far the most time-consuming submodel. This submodel predicts the photosynthetically active radiation (PAR) intercepted by each plant of the crop:weed canopy volume discretised into voxels (3D pixels). It used 57%, 64% and 99% of total simulation time with a voxel edge size of 7, 4 and 1 cm, respectively. The second most time-consuming submodel was the germination/emergence submodel which used 20%, 7% and 0.04% of the computation time for the three voxel edge sizes. Consequently, we will focus here on simplifying and accelerating the radiation interception submodel.

2.3 A short presentation of the 3D radiation interception submodel

The 3D radiation interception submodel (Munier-Jolain *et al.*, 2013) simulates a 3D sample of the virtual field where the space is discretised into voxels (i.e. 3D pixels). Crop and weed plants are placed onto this field, with plant position and morphology resulting from other FLORSYS submodels. Crop plants can be sown in rows or broadcast (*i.e.* random position in the field); weeds can be positioned randomly or in species-specific patches. The radiation interception submodel calculates the amount of photosynthetically active radiation (PAR) that arrives on top of the crop:weed canopy and that trickles down to the voxels in the underlying layers, depending on plant leaf areas, species radiation extinction coefficients and solar angle (which depends on latitude and season). In total 14 input variables can be modified in the submodel for five different outputs.

2.3.1 3D radiation interception inputs

Plants are represented as cylinders delimited by their height and width (Figure 2, Table 2.A). The leaf area (LA) of the plant is distributed across the successive voxel layers of the cylinder, with 50% of the cumulative leaf area below relative median leaf height (RH50) of the plant and its distribution governed by the shape parameter, b. The species radiation extinction coefficient (k) and the plant leaf area inside each voxel determine how much incident radiation of the voxel is absorbed by the plant's leaves. The radiation absorbed by each plant (PARa) is the sum of the radiation absorbed by its leaves in the different voxels. Other inputs describe the location: (1) the field sample, *i.e.* dimensions in the north-south and in the east-west directions, as well as the grain of the discretization, *i.e.*, the voxel edge size, and (2) the position of the solar angle, *i.e.* latitude of the simulated field and the Julian day.

2.3.2 3D radiation interception outputs

Outputs of this submodel (Table 2.B) are used for different purposes in FLORSYS: the photosynthetically active radiation absorbed by a plant (PARaP) drives biomass accumulation in the growth submodel, the daily shading intensity perceived by the plant (SID) drives etiolation in the morphology submodel. The relative intercepted photosynthetically active radiation (rPARi) is considered at three scales, the top of a given plant ($rPARi_{top}$), over the whole plant ($rPARi_{plant}$), and the soil surface below all plants ($rPARi_{base}$). These are used as proxies for herbicide penetration and interception in the canopy in the herbicide treatment submodel.

As single plants are not shaded by neighbouring plants, their relative PAR intercepted on the plant's top ($rPARi_{top}$) is always 1.Thus, for the single plant case, only four outputs were studied, *i.e.* PARaP, SID, $rPARi_{plant}$, $rPARi_{base}$. For the "plant in a canopy" step, all five outputs are studied (Table 2.B). The metamodels also predict PARa per cm² (PARaC), *i.e.* relative absorption efficiency for a given plant volume.

3 Simplification and acceleration of the 3D radiation interception submodel

To find the best metamodelling and sensitivity analysis method for the radiation-interception submodel, we started with the simplest possible situation for this submodel which consists of a single plant in a field, without shade due to surrounding plants (step 2 in Figure 1). Once identified, this method was then applied to more realistic but more complex occurrences relevant for the submodel, *i.e.* target plants surrounded by neighbour plants (step 3 in Figure 1).

3.1 Simplified case study with single target plants (step 2)

This section aims (1) to test the effect of the range of variation in inputs, (2) to test the effect of correlations between inputs, (3) to analyse the sensitivity indices for unshaded (single) plants, and (4) to evaluate the metamodels predicting the radiation interception variables for unshaded plants.

3.1.1 Testing the sensitivity to the range of the inputs (step 2.i)

Two input range sizes were tested following a Plackett & Burman experimental design (Plackett and Burman, 1946) with 12 combinations of the two extreme ranges for the 11 inputs with Latin Hypercube Sampling (LHS) designs of 29200 rows (supplementary material online S2 section 1): (1) a small range corresponding to France, focusing on spring and summer, and the plant morphologies most common in fields and (2) a large range for all possible plant morphologies growing, all year and all around the world (except polar regions). For each configuration of ranges, the FLORSYS radiation interception submodel was run with a single target plant located at the center of the field sample, and Sobol sensitivity indices (Saltelli, 2002) were estimated for the analysed outputs. Sobol indices are the most widely used sensitivity indices and are robust enough for complex models (Gauchi et al., 2017).

The Sobol decomposition leads to decompose the variance of a on-linear model output into percentages of variance which can be attributed to the different inputs, discriminating the variance due to the main effect of a given input from the one resulting from interactions with other inputs. The Sobol indices, based on these variance percentages can be directly interpreted as measures of sensitivity measured across the whole input space. The main advantages is that Sobol indices can deal with nonlinear responses and interactions in non-additive systems. This design gave a set of 12 sensitivity indices for each of the 11 inputs. A linear regression of these sensitivity indices was fitted, where the regression coefficients indicate the importance of the effect of the range.

Absolute values and ranking of sensitivity indices of the various inputs changed for all outputs when a small input range was used instead of large one (supplementary material online S2 section 1). Not all inputs were, though, concerned, depending on the analysed output, *e.g.* the range of the voxel was important for the relative intercepted PAR (PARi) but not for the shading index (SID). Consequently, for the subsequent steps, the large input ranges were used to cover all the possible input situations and notably for novel combinations of species traits, *e.g.* resulting from new crop varieties or invasive weed species.

3.1.2 Sensitivity indices estimation via Sobol-Saltelli method and via Polynomial Chaos Expansion

The objective of this section was to compare the Sobol sensitivity indices that we estimated in section 3.1.1 with a method that both estimates sensitivity indices and fits a metamodel. The Polynomial Chaos Expansion (PCE) method uses the same principle as Sobol sensitivity indices *via* Ordinary Least Square Regression (Sudret, 2008), here shortened to PCE-OLS. For each input, the sensitivity indices estimated by the polynomial chaos expansion are (1) the polynomial effect that accounts for the effect of the input only (*i.e.* the main effect of the input) and (2) the total effect (*i.e.* quantifying all the interactions of this input with other inputs). These indices are respectively comparable to the first-order indices and the total-effect indices of Sobol indices. The large-range experimental design *via* Latin Hypercube Sampling, LHS (McKay et al., 2000), created in the previous section was used to estimate both indices. PCE-OLS indices were similar to Sobol indices computed on the same dataset (supplementary material online S2 section 2). The largest difference was of 0.13 for the total effect of the voxel on the radiation intercepted by the target plant ($rPARi_{plant}$). The ranking of the inputs was the same with both methods. We thus preferred PCE in the following steps since it both estimates sensitivity indices and fits a metamodel, which is needed to simplify the radiation interception submodel.

3.1.3 Sensitivity indices with correlated inputs (step 2.ii)

The method for estimating PCE-OLS indices assumes that inputs are independent and uncorrelated. However, some inputs of the radiation interception submodel are correlated, *e.g.* plant height and the

total leaf area are strongly linked (*e.g. Galium aparine L.* (Klem et al., 2014)). We thus tested the effect of including correlations among inputs on the estimation of the sensitivity indices and decided whether the method needed to be adapted. This part was fully presented in Gauchi *et al.* (2017) and further details can be found in supplementary material online S2. In summary, the space filling LHS design of section 3.1.1 was modified to include correlations among inputs following the Iman and Conover method (Iman and Conover, 1982). These correlations (supplementary material online S2 section 3) were estimated on simulated plants occurring in 10 diverse cropping systems (Colbach et al., 2016b). A number of 10000 runs were selected out of a total of 29200 runs to avoid an excessive weight of outputs too close to the limit of the ranges. We ensured that the experimental design remained orthogonal and that enough runs were kept to estimate the sensitivity indices. Adding correlations to the space filling design of the inputs changed absolute values of sensitivity indices PCE-OLS for all outputs and gave deviant values (< 0 or > 1).

Consequently, it was essential to find a method better adapted to correlated inputs. Gauchi *et al.* (2017) proposed to calculate the sensitivity indices (*i.e.* polynomial effect and total effect) by estimating the coefficients of Polynomial Chaos Expansion using a Partial Least Squares method, namely a Partial Least Squares Regression (PCE-PLS, see (Wold et al., 2001)). Here, the resulting PCE metamodels were though too complex to speed up FLORSYS computations. We thus built more parsimonious and faster metamodels, using a method developed by Gauchi et al (2017) who tested it on a single FLORSYS output. These parsimonious faster metamodels were built with a LASSO regression (Tibshirani, 1996) to select monomials via GLMSELECT (SAS). With the selected monomials we performed a new PLS regression for the final parsimonious metamodel (hence, "fast" metamodel). This combination of methods was hence referred to as LASSO-PLS. The resulting single plant PCE-PLS metamodels (full and fast) were evaluated via a PLS specific criterion, the Q^2_{cum} (Tenenhaus, 1998; Lazraq et al., 2003) for fitting and prediction qualities. We used the same principle and stopping rule as in Gauchi *et al.* (2017) giving a $Q^2_{cum}(h^*)$ referred to as Q2cum in this paper. This cross-validated fitting prediction criterion is bounded between 0 and 1; the closer to 1 it is, the better the metamodel is in terms of prediction and fitting. The prediction error was evaluated via the relative mean squared error in predicton RRMSEP (supplementary material online S5 section 1). This method was used for the sensitivity analysis and metamodelling of the single-plant case (sections3.1.5) and then for the more complex case with target plants surrounded by neighbouring plants (section3.2).

3.1.4 Identifying the key inputs that drive radiation interception of single plants (step 2.iii)

The sensitivity analysis based on PCE-PLS showed that that the most important inputs for the photosynthetically active radiation absorbed by the plant (PARaP, which drives plant growth) were voxel size and plant width (Figure 3). The third most important inputs were the target-plant characteristics driving potential leaf area absorption ability, *i.e.* total plant leaf area and species

extinction coefficient. Total leaf area and plant volume (determined by its width and height) affected PARaP more than leaf distribution (RH50 and b). The environmental variables (latitude and day) as well as field size had small but non-negligible impacts. All inputs strongly interacted, with interactions making up between 46 % (voxel edge size) and almost 100% of the total effect (all others except plant width). Consequently, the sign of the main regression coefficient of an input was useless to assess how an output varied with an input. Graphs of outputs vs. inputs confirmed that interactions made it usually impossible to identify general tendencies, except that PARaP tended to decrease with increasing plant height and width, indicating a self-shading effect (supplementary material online S2, Figure 2 in section 5).

The same general tendencies as for PARaP were observed for the other outputs, *i.e.* all inputs matter, voxel edge size and target plant variables mattered more than physical variables and field size (though voxel size could be less important for some outputs such as the shading index, SID); plant volume (though the most relevant variable could be height rather than volume) and leaf area mattered more than plant shape and leaf distribution (supplementary material online S2 section 4).

This analysis also showed that large voxel edge sizes (i.e., 10 cm and above) frequently led to weird outputs values, such as an abnormal concentration of 0.5 values for the $rPARi_{plant}$ (supplementary material online S2 section 5). This is due to the computational effect of the voxel-based algorithms, notably when voxels are so large that they include the whole plant (further details in supplementary material online S2 section 5). For small voxels, this only occurs during the 1-2 days after plant emergence, at a time when shading and light absorption have no influence on later plant growth because young plants do not respond to shading and their biomass accumulation only depends on temperature in FLORSYS.

3.1.5 Metamodels for a single plant (step 2.iv)

The metamodels for a single target plant in the field included all inputs as the sensitivity analysis indicated that all were influential, albeit to varying degrees. The full metamodels included 4367 monomials resulting in a good (*i.e.* close to 1) Q2cum (0.93 - 0.98) (Table 3.A, lines 1, 3, 5, 7) and a low prediction error (RRMSEP = 0.15 – 0.25 $MJ \cdot MJ^{-1}$) (supplementary material online S5 section 3). LASSO-PLS selection produced simpler and faster metamodels, with only 25 to 27 monomials, resulting in a quite good Q2cum (0.70 - 0.90) but a slightly worse prediction error (RRMSEP = 0.35 – 0.55, Table 3.A, lines 2, 4, 6, 8). Regardless of the metamodelling approach (fast or full), radiation interception at the base of the target plant ($rPARi_{base}$, a proxy for the total herbicide penetration into the canopy) is the least well predicted output. This was also the only output that was not calculated at the scale of the plant but at the field scale.

3.1.6 Summary for single target plants

We tested different sensitivity-analysis methods that increased our knowledge of the 3D radiation interception submodel. This resulted in a more appropriate method that accounted for the correlated inputs. We then proposed a handy solution for more parsimonious and faster metamodels. Part of the methods were developed in a previous study on a single output (Gauchi et al., 2017) and were completed here before being applied to a larger set of outputs.

3.2 Case for a target plant inside a canopy (step 3)

Fields (or even field portions) rarely only comprise a single plant. Step 4 thus focused on radiation interception of target plants surrounded by neighbouring plants. The method developed in the previous step to analyse and metamodel radiation interception from target-plant, environmental and precision inputs was adapted to (1) include contrasting canopies representing the diversity in crop:weed canopies in arable fields in the simulation plan while (2) limiting the amount of additional inputs needed to describe the canopy surrounding the target plant.

3.2.1 Simulation plan

A canopy is a complex set of plants of different species, sizes, widths, positions, etc. To set up diverse plant canopies in our virtual field, we needed to vary many variables: plant density (crop density, weed density, amount of bare field area), the position of weeds (random or in patches, number of patches in the field), the position of crop plants (row vs broadcast sown, inter-row width), canopy structure (e.g., presence and diameter of canopy gaps surrounding target plants), the heterogeneity of plant morphology (mean and variation coefficient of target plant characteristics), weed populations being more heterogeneous than crop population (*i.e.* presenting a larger range of variation) (see supplementary material online S3). These preliminary inputs were used in a LHS design of 20440 rows. Correlations were added in the same way as for the single-plant study, with the Iman and Conover method (Iman and Conover, 1982). The diverse canopies were built by placing the plants on a virtual field and attributing morphologies, and then radiation interception and absorption were simulated with the FLORSYS radiation interception submodel. Cases with outlying values were removed as well as output values too close to the range limits (*i.e.* 0, 1 or 100 depending on the output) to avoid side effects due to computation errors; 2536 canopies remained after the sorting. The PCE-PLS method was used to metamodel and perform the sensitivity analysis.

3.2.2 Describing the canopy

Many detailed variables are needed to create contrasting canopies in FLORSYS, but only a limited number of inputs are allowed keeping the metamodel simple. The detailed canopy variables were thus aggregated into five mean canopy inputs (Table 2), to account for the canopy effect in the metamodel. The nearer the neighbours are to the target, the more their characteristics contribute to the variables describing the average canopy characteristics, here the example of the canopy height (cm):

Eq. 1 $$mean\ height = \frac{\sum_{i=1}^{n}(\frac{1}{d_i+1} height_i)}{\sum_{i=1}^{n}(\frac{1}{d_i+1})}$$

where d_i is the distance (m) of the target plant to the closest neighbour plant i (+1 to account for a zero distance when the neighbour is located in the same voxel as the target), $height_i$ is the height (cm) of neighbour i and n the number of neighbour plants in the field sample. For the equations of the other canopy variables, see supplementary material online S3 section 4.

In addition to these aggregated canopy inputs, we added: (1) the plant density and the maximum distance between the target plant and neighbour plants, (2) target plant variables (as in the single plant case) and (3) two environmental variables (latitude and day), resulting in 15 metamodel inputs (Table 2). To reduce the number of inputs, field dimensions (Xmax and Ymax) whose effect was shown to be slight in the single-plant sensitivity analysis of the single plant (section 3.1.4) were both fixed at 8 m which allowed having large plants in the virtual field sample. The voxel size was shown to be important for most outputs (section 3.1.4), but to simplify and accelerate the simulation plan, we kept it constant. Additional simulations (supplementary material online S2 section 6) showed that a voxel edge size of 4 cm was the best compromise between the precision of the radiation interception submodel output and the computation time.

3.2.3 Sensitivity indices (step 3.i)

The sensitivity analysis of radiation interception outputs to inputs depicting target plant, physical environment and neighbour plants showed that input effects were almost entirely due to interactions among inputs (Figure 4). Globally, target-plant inputs had the most and neighbour-plant inputs the least impact. Inputs of a given type had similar effects, except for the relative PAR intercepted by the target plant ($rPARi_{plant}$) whose height effect was several times the effect of any other inputs. As for the single-plant scenario (section 3.1.4), the interactions among inputs were generally too complex to identify general tendencies, whether from the signs of the polynomial effects or from graphs (supplementary material online S2 section 5). And again, outputs were sensitive to all inputs *via* interactions with other inputs and none of latter could be set at a default value in the following metamodels.

3.2.4 Metamodels (step 3.ii)

The metamodels for target plants surrounded by neighbour plants included all inputs, *i.e.* for describing the target plant, the physical environment and the biological environment due to the neighbour plants. The polynomial degree of these metamodels was smaller than for the single-plant ones, except for the relative intercepted PAR rPARi, (Table 3.B, lines 14-15); the Q2cum was always lower and the prediction error higher (Table 3.B vs A). Further increasing the polynomial degree did not improve the Q2cum or reduce the prediction error (results not shown). The need for a higher polynomial degree for the rPARi points to more and more complex interactions among inputs. The fast

metamodels usually needed a higher polynomial degree and more complex monomials (Table 3.B) than full metamodels to optimize the Q2cum. The latter though remained low (0.27-0.56) and prediction error was much larger than for single plants (0.85 and 0.65). Radiation interception and absorption by a plant surrounded by neighbour plants is thus much harder to simplify *via* a small metamodel than for single plants.

3.2.5 Summary for plants in the canopy

The metamodels for radiation interception and absorption by a plant surrounded by neighbour plants were simple enough to be implemented into FLORSYS but with a poorer prediction quality than for a single plant. The canopy creates a complex interaction with the radiation that cannot be easily simplified at a scale as large as the plant. Strong interactions between all inputs prevented us from setting the least important inputs to constants.

4 Combining the metamodels into a FLORSYS submodel (step 4)

As we had developed metamodels for two situations, *i.e.* single plant and plant in a canopy, it was necessary to establish rules to determine when to use which metamodel in a simulation using the whole FLORSYS including the metamodels (hereafter called FLORSYS-ML). This section presents how the metamodels were combined and what else was needed to cover all likely canopy scenarios with FLORSYS-ML.

4.1 Principle

Even when there is more than one plant in a field, some of these plants can be considered as single if they do not interfere with each other's radiation interception, which depends on plant sizes, solar angle and distance between plants. Consequently, each day, for each target plant (crop or weed), rules are needed to determine whether a target plant can be considered as single or as surrounded by neighbour plants (supplementary material online S4 section 2).

When building the metamodels, a large number of runs were eliminated because outputs were too close to the limits of the range or because their combination was biologically impossible and resulted in deviant values (section 3.2.1). This also reduced the ranges accepted by the metamodels for several key inputs such as target leaf area, making it impossible to predict radiation interception for newly emerged seedlings (*i.e.* with almost nil height, width and leaf area), voluminous single plants (having reached the maximum height and width possible for the species) or mature plants with dried leaves (with a near zero leaf area). But such plant morphologies are frequent in any cropping system. To remedy this, further metamodels were built for the particular case of small seedlings, and for the remaining outlying situations, equations were added to predict radiation interception and absorption from ecophysiological knowledge, or from likely constants (section 4.3). Figure 6 summarizes how the

different rules, equations and metamodels were aggregated. Finally, the calculation loops over neighbour plants needed to calculate the aggregated canopy variables are often time-consuming. As a consequence, alternative methods to compute aggregated neighbour were tested (section 4.4).

4.2 Rules for deciding whether to use the single plant or plant in a canopy metamodel

4.2.1 Method

The PAR intercepted at the top of a target plant ($rPARi_{top}$) is relevant to identify whether radiation interception by the target plant is impacted by neighbour plants, because this output is always 1 for single targets and decreases in the presence of shading neighbours. To establish decision rules to discriminate these two situations, a regression tree was built from the data sets of sections 3.1 and 3.2, using the inputs listed in Table 2. As the metamodels in the previous sections showed that it was difficult to take account of all effects and interactions with these inputs, some were transformed and others added in the present analysis. The environmental variables were transformed to emphasize the effect related to solar angle: latitude was transformed into degrees to the equator (*i.e.* absolute latitude) and Julian days into days from the summer solstice to the winter solstice (*i.e.* between solstice days). The distance from target plant to its closest neighbour was also used as input (with distances calculated between plant centres), and all other inputs were weighted by the inverse of this distance to take into account that closer neighbours shade more than farther neighbours. Finally, the target height relative to the canopy height (overtaking percentage) was integrated *via* the ratio of the difference between the two heights (eq. 6 supplementary material online S3 section 5).

The CART method (Breiman et al., 1984) was used to build a classification tree to determine the decision rules. This method successively splits the data set into two subsets along a threshold value of an input (*e.g.* distance to the closest neighbour) in order to maximize the difference between subsets in terms of output. Branches are combinations of input values that lead to output predictions contained in leaf nodes. CART also ranks the input according to their importance to explain the output.

The output analysed in the trees was not directly the $rPARi_{top}$ but a binary variable indicating whether the target plant was considered single or inside canopy, depending on whether its $rPARi_{top}$ was respectively $\geq$ or $<$ a threshold value. In addition to the theoretical value of 1, ten other thresholds were tested, ranging from 0.90 to 0.99 (incremented by 0.01), in order to increase the number of single plant cases compared to canopy cases and thus the robustness of the tree. Among the 11 trees, the one corresponding to the 0.98 threshold was chosen. This threshold is close to 1 (i.e. the theoretical value of $rPARi_{top}$ in single plants) and it identified the most situations when to use the single-plant metamodel. The latter allows accelerating calculations because the single-plant metamodels were simpler and did not need to calculate the aggregated canopy variables.

4.2.2 Decision tree to determine where a target is shaded by neighbours

The rules determining whether a target plant can be considered as single are shown in Figure 5. For example, if the nearest neighbour is further than 1.6 m, and the target plant is taller than the neighbouring canopy, the target can be considered as single. Surrogates of the tree (*i.e.* variables correlated to the variable in the tree that could also explain the segmentation, but to a lesser degree) and ranking of variables in their order of importance (supplementary material online S3 section 6) showed that nearest neighbour distance (either alone or in interaction with other variables) are predominant to determine whether the target plant is single or within a canopy.

Based on expertise, we added a further logical rule: if there are no neighbours whose height exceeds the distance separating the outer rims of the neighbour and target plants, the target is considered as single. In that case, even if the sun is low on the horizon, the closest neighbour is too far to shade the target (supplementary material online S4). The combination of the decision tree and this additional rule constitute step A in Figure 6.

4.3 Adding equations at the limits of the input ranges

The input ranges of the metamodels missed small seedlings for which good prediction is essential as their initial growth determines which plants outgrow the others. Consequently, we ran a further simulation plan to build a third metamodel focusing on small seedlings (Step C, Figure 6), using the method developed in section 3 (supplementary material online S4 section 4). This additional metamodel was still inadequate for fresh seedlings whose leaf area was lower than the metamodel's accepted input range. In that case, as there is neither shading nor self-shading, the PARa absorbed by the plant is the product of the incident PARa, the plant leaf area times its extinction coefficient, based on Beer's law (Monsi and Saeki, 1953, 2005) (step B in Figure 6). This works fine for single plants that are unshaded by neighbours. To include either small plants surrounded by neighbours or any plants by small neighbours outside the canopy metamodel range, a linear combination of predictions for single plants (either small or large) and plants in canopy was used, step G in Figure 6. This was particularly true for canopy leaf area whose lower range limit was extremely high (Table 2). Single-plant predictions and target-in-canopy predictions were weighted by respectively 1 and the canopy leaf area, and divided by the same of these weights (supplementary material online S4 section 4).

The metamodels do not include voluminous or mature leaf-less plants either. As these have finished their growth, outputs were simply fixed either to a minimum or maximum value, or linked with a simple regression if one input was out-of-range (step Figure 6). The values were based on graphs of outputs *vs.* inputs from the complete data set including the outliers that were ousted during metamodel construction (supplementary material online S4 section 4). If several inputs were out of range, the output was estimated based on the analysis of the most influential input, with the strongest polynomial

effect in the sensitivity analysis (supplementary material online S4 section 4). For example, if a target plant surrounded by neighbours is taller than 254.8 cm, then its relative intercepted PAR is 0.00649 $MJ \cdot MJ^{-1}$.

4.4 Different methods to aggregate neighbour plants into canopy variables

We proposed three different methods to calculate the aggregated neighbour variables of each target plants: (1) all neighbours close to the target are used for the computation ("local" neighbours), (2) all plants in the field are averaged and the same aggregated variables were used for all target plants ("average" neighbours), (3) a mix between the previous two methods, using average canopy variables when the plant density exceeds 500 $plants.m^{-2}$, and local neighbours otherwise. The effect of the aggregation method on prediction error and simulation speed of the whole FLORSYS-ML was evaluated in section 5.

5 Evaluation of the simplified FLORSYS-ML with field observations (step 5)

5.1 Objective

Sections 3.1.5 and 3.2.4 evaluated the prediction quality of the individual metamodels. Here, the objective was to evaluate how good and fast the predictions produced by FLORSYS-ML compared to the process-based FLORSYS, by comparing simulations to field observations following the methods developed in a previous paper (Colbach et al., 2016b). Different voxel edge sizes and the three methods for aggregating neighbour plants were tested.

5.2 Material and methods

5.2.1 Field observations and features common to all simulations

Observations were taken from the INRAE long-term field experiment at Dijon-Epoisses (Burgundy) (Chikowo et al., 2009) where weed and crop variables (plant and seed densities, plant biomass, yield) were monitored from 1999 to 2012. Details can be found in (Colbach et al., 2016b). This trial included ten fields with diverse crop rotations, ranging from intensive herbicide-based to herbicide-free systems and varying degrees of tillage and mechanical weeding. Weed flora was assessed, with species identification, plant density, above-ground biomass and seed bank measurements. Crop yield was also estimated.

5.2.2 Simulation plan

The simulation combined (1) the FLORSYS version (metamodelled or process-based), with (2) the voxel edge size (1, 4 or 7 cm) which determined the precision of plant location (all FLORSYS versions) and plant morphology (processed-based version). The FLORSYS-ML version moreover tested

(3) different methods for aggregating neighbour plants (local, average, or mixed, see section 4.4), and the process-based version tested (4) field sample areas (1m × 1 m, 3 m × 3 m, and 6 m × 3 m) with a 7-cm voxel. Unless otherwise indicated, field area was 6 m × 3 m. In total, nine scenarios were run with the FLORSYS-ML version and six with the process-based one. Each of the ten field histories was simulated over 13 years, using the weather measured at the local weather station (INRAE Climatik platform) and starting with the weed seed bank observed at the onset of the field experiment. Each scenario was repeated ten times, to account for stochastic effects. Outputs were produced for all the days where observations were carried out in the fields. Simulations were run with a computer with two 2GHz processors and 16 Gb RAM and their simulation time was recorded and averaged over repetitions for the different methods.

5.2.3 Evaluation criteria

Simulations with the metamodelled FLORSYS-ML and process-based FLORSYS were compared to field observations. Prediction error was assessed with the relative root square mean squared error of prediction (RRMSEP) corrected for variability in observations (due to measurement errors and intra-field variability) and simulations (due to stochasticity) (Colbach et al., 2016b). This error was calculated relative to the range of variation of the observations (details can be found in supplementary material online S5 section 1). Outputs were analysed at two temporal scales, either corresponding to the individual observation dates (daily scale), or values averaged over the simulation (multiannual scale).

5.3 Results

5.3.1 Mean simulation time

The simulation time of the process based FLORSYS for all cropping systems tested, decreased with voxel edge size. When voxel edge size increased from 1 to 4 cm, simulation time was divided by approximately 20 (Figure 7.A). Increasing voxel size further from 4 to 7 cm decreased simulation time by an additional 43%. Increasing voxel size from 7 to 10 cm did not decrease simulation time any further. The slowest scenario took 259 times more time than the fastest. The fastest scenario with the 7 cm voxel edge size and 1-m² field sample took 4 minutes for a repetition of the 13 year long cropping system, compared to more than 18 hours for the slowest, with the 1-cm voxel and the 18-m² area. Conversely, simulation time increased with field sample area (supplementary material online S5 section 2). Increasing area from 1 to 9 m² multiplied the simulation time by approximately 8; doubling the field sample area to 18 m² only increased the simulation time by a further 10%. The field size multiplies the simulation time by 1.15 for every m² of a 13-year simulation

The simulation time of FLORSYS-ML remained stable for all voxel sizes, but it depended on the method for calculating neighbouring canopy variables (Figure 7.A). The FLORSYS-ML with average neighbours was fastest and the one combining local and average neighbours was nearly as fast.

Always using local neighbours made simulations considerably slower than with the process-based model, and simulation time even increased with voxel edge size. Indeed, in FLORSYS-ML, the voxel determines plant location, and the larger the voxel is, the more plants are in each voxel. So, when FLORSYS-ML searches through the voxels surrounding the target plant to compute the canopy inputs, it must compute more plants, which takes longer. FLORSYS-ML was considerably faster than the process-based model with small voxel edge sizes, *i.e.* 28 times faster for FLORSYS-ML with average neighbours.

5.3.2 Prediction error

In process-based simulations, the prediction error tended to increase slightly with increasing voxel size (Figure 7.B). The same trend was observed for prediction error in FLORSYS-ML simulations with larger voxels, suggesting a sensitivity to plant position, which is less precise if the voxel is large. Simulations with a 1-m² field sample produced slightly better results than 18-m² and larger areas (*e.g.* for the multiannual weed density for all species summed, the RRMSEP for 1×1, 3×3 and 6×3 m² field samples was respectively 63, 113 and 116 $MJ \cdot MJ^{-1}$, details in supplementary material online S5 section 3), probably because it increased interspecific competition between weed species by increasing the probability of overlapping species patches. However, small fields potentially miss rare species, and overestimate interspecific competition in case of high weed densities.

Generally, the error was larger for metamodel-based vs. process-based simulations, particularly for weed plant biomass (Table 4), and it varied more among repetitions (supplementary material online S5 section 3). Error was often smaller than the variability in observations, pointing to a negligible prediction error, and making it impossible to calculate the relative variation in error for metamodelled vs process-based simulations (Table 4). Conversely, FLORSYS-ML was better than the process-based FLORSYS to predict multiannual weed plant densities.

Usually, FLORSYS-ML using either local or average neighbours respectively had the smallest and largest errors, whereas errors were intermediate when using both average and local neighbours (Figure 7.B, Table 4). Regardless of the evaluation criteria, there was no model version (process or metamodel-based, approach for calculating canopy variables in metamodels) or precision level (voxel size, field sample area) that optimized the precision of all model outputs.

6 Discussion

6.1 Simplifying a complex process-based model

In this article, we presented a method to accelerate and simplify a complex process-based model. The paper is of interest for non-statisticians that want to metamodel complex models and are often baffled by statistical methods and how to apply them in their real-life complicated situation. Another particularity of our work was that we did not use the metamodel as such but integrated it into a larger

model and evaluated the latter with independent field data, two steps that have, to the best of our knowledge, been rarely carried out in the past.

From a more technical point of view, the originality of the approach lies in (1) the choice of metamodelling only the most time-consuming part of the model (*i.e.* the 3D light-interception submodel), (2) the choice of an innovative metamodelling method that handles correlated inputs and selects monomials, (3) the integration of the metamodelled submodel into the complex model and (4) the description of the nearby canopy with a limited number of inputs. This work did not compare different metamodelling methods (Villa-Vialaneix et al., 2012) but provided practical guidelines for choosing and tuning metamodelling methods with respect to the complex model constraints (*e.g.* correlated inputs). It extended what was done in the previous paper (Gauchi et al., 2017) by showing the whole approach to simplify a complex model. Usually, metamodelling via polynomial chaos expansion allows reducing the number of inputs in the model by setting the inputs to average values (Luo et al., 2013; Rothenberg and Wang, 2016). Here, however, no input could be omitted because all either influenced radiation interception outputs directly or in interaction with other inputs.

Usually, the whole model is metamodelled, avoiding the need to integrate the metamodel into a larger model (Cohen and Prinn, 2011; Luo et al., 2013). Here, we metamodelled a single time-consuming submodel in order to accelerate the simulations of the whole FLORSYS model, and we thus had to integrate the metamodels, together with complementary equations, into FLORSYS. In SIRIUS (Brooks et al., 2001), only a few equations were metamodelled. No implementation of the metamodel was needed, as the metamodel was as good as the whole SIRIUS to predict the yield, which was the study's goal. The constraints of this approach were manageable for the 3D radiation interception of FLORSYS even though the number of inputs needed to be decreased with the help of aggregated canopy variables. But these constraints probably make it impossible to apply this metamodelling method to bigger models like the whole FLORSYS with its many more inputs and correlations.

6.2 Experimental design for analysing a complex model

The numerical space filling design, Latin Hypercube Sampling (LHS), is usually appropriate to explore the whole space of possible input combinations. For our biological example, we also used the Iman and Conover method (Iman and Conover, 1982) to apply a correlation matrix to the LHS, to increase the biologically realistic plant variable combination. It worked less well for the dynamic FLORSYS model, especially at the outer bounds of input ranges that were not sampled enough, despite having tested the best minimum row number in the LHS design. This was particularly problematic at the onset of the plants' life-cycle (*i.e.* for small plants) as imprecise early predictions would amplify the next days' prediction errors, thus setting off the plants' growth and development in entirely the wrong direction. We improved the metamodelling by using separate experimental sampling designs, combining with a simplified process-based approach, discriminating three types of plants that differ in

terms of light interception, based on their age and size: (1) a standard LHS and metamodel covering mostly large and older plants, (2) a second LHS and metamodel specifically targeting younger smaller plants, (3) a simplified ecophysiological equation for newly emerged tiny plants. The latter approach was acceptable here as these plants do not self-shade and are rarely shaded by neighbours. No such effort was made at the other extreme of plant-size range, i.e. large adult plants with dried leaves. Indeed, these do not photosynthesize anymore and misestimating their absorbed light would have little impact on their future. Colleagues aiming to similarly metamodel complex could use a similar approach, i.e. keep a process-based (albeit simplified) approach for the most sensitive stages/components (here, the newly emerged tiny plants) and combine separate sampling plants and metamodels to ensure that the more sensitive stages/components are adequately covered (here, the small plants).

The inability of the metamodels to correctly predict small plants is explained by three combined reasons: (1) we chose a broad input range to cover all possible plant morphologies in the field, which reduced the probability of drawing many low input variables, (2) as the simulated plants were the combination of several inputs, the probability of drawing a small plant combining low values of all inputs (*e.g.* low height, width and leaf area) was even lower, particularly as the space filling design was balanced, (3) the equilibrated design also drew plants combining high values for some inputs with low values for others, resulting in biological impossible morphologies (*e.g.* tiny plants with an enormous leaf area) and non-logical output values. These plants had to be removed from the data set, decreasing even more the occurrence of extreme input values used in the metamodels. For models with a high number of inputs it is thus better to sample stepwise rather than have a unique sampling design. Surprisingly, adding correlation to inputs did not help to ensure many small and plausible plants.

6.3 Which method for which application?

To metamodel and perform a sensitivity analysis, many methods exists, which have been assessed in comparative studies. We thus decided to detail here the entire path when choosing and applying a method to transform a complex slow model into a faster metamodel. Polynomial chaos metamodelling accepts only a small number of inputs, hence the aggregation of neighbour plant variables into a small number of synthetic canopy variables. Unfortunately, it is the aggregation step, particularly the loop computing the plants close to the target plant, which cancelled out the simulation time saved thanks to the metamodels.

Another way to speed up simulations would be to use the initial process-based interception submodel and to decrease the precision of the canopy structure by increasing the voxel edge size, which governs the precision of plant locations and volumes as well as leaf distribution along plant height. This approach led to less precision loss than expected. Indeed, FLORSYS does not explicitly represent plant architecture in detail, with each organ (e.g., leaf, stem) simulated. If that had been the case, enlarging

voxels would indeed decrease prediction quality considerably. Actually, FLORSYS distributes leaf area in voxel layers, without considering leaf size, position or inclination. Very small voxels do thus not necessarily place leaf area in the correct voxel layer and downsizing voxels cannot be simply approximated here to differential equations that govern light transmission. We already discussed the fact that model quality does not decrease below a certain voxel size and is not best for the smallest voxel (i.e. the highest precision) in Munier-Jolain et al (2013). Moreover, there are several stochastic functions in FLORSYS, particularly for plant location in the canopy. This explains why differences between scenarios differing solely in terms of voxel size are not solely due to differences in voxel size.

We thus identified two ways to save simulation time depending on the simulation goal: either by decreasing the precision of the plant and canopy description (process-based light interception submodel with a large voxel edge size) or that of the light interception (metamodelled submodel with a small voxel edge size). Choosing rapidity over precision can be appropriate, for example when needing quick simulations for workshops with farmers to co-design cropping systems (Bergez et al., 2010). The choice of the approach then depends on the target output (Table 5). When plant location is essential (e.g., when testing site-specific weed management, small sowing interrows, row-only nitrogen fertilization) (Berge et al., 2013), then a voxel size of 1 cm is needed, and the metamodelled FLORSYS-ML would allow faster and thus more simulations than the process-based FLORSYS. When both moderate simulation time and prediction quality are needed, the process based FLORSYS with a voxel size of 4 cm would be best. For cropping system tests, a quantitative precision is less essential as long as the management recommendations are correct (Renton, 2011).

6.4 What other solutions to speed up a complex model?

Instead of only simplifying the process-based approach for tiny newly-emerged plants, we also thought about using a simplifying process-based light interception model. This approach was used in early crop-weed competition models (Graf et al., 1990; SOYWEED: Wilkerson et al., 1990; ALMANAC: Kiniry et al., 1992; e.g. INTERCOM: Kropff and Spitters, 1992; Kropff et al., 1992) as well as in intercrop models (Gaudio et al., 2019). However, these models only work for homogeneous 2-species canopies and cannot grasp the complexity of heterogeneous multispecies crop-weed canopies (in terms of location, emergence timing and morphology), as shown by comparisons of simulations with such models to independent field observations (Debaeke et al., 1997; Deen et al., 2003). Consequently, the recent trend in crop-weed competition modelling goes towards more complexity rather than less (Renton, 2013). A recent review of multispecies canopy models even concluded that the FLORSYS approach was a good compromise between simplicity and accounting for canopy heterogeneity (Gaudio et al., 2019).

There are also technical solutions for speeding up simulations, for instance parallelising the execution of the source code or using graphical processing units. Unfortunately, these solutions make it difficult

to maintain a unique source code for any type of computer or server. A "portable" solution is to run multiple FLORSYS clones simultaneously on a single computer or server, either manually or automatically via scripts. The speed gain then depends on the number of logical processors of the computer. Another avenue is similar to the large-voxel solution, i.e. reduce the size of the simulated field sample. This solution was already assessed in a previous paper (Colbach et al., 2016b) where we determined the minimum acceptable size. Again, the more complex (e.g., many species, large interrows), the larger the field sample needs to be.

So, there are several avenues for speeding up a complex model (Table 6). The best choice depends on the objective and situation of use, and several solutions can be combined for an even better result.

6.5 Towards a larger simplification of FLORSYS

The simplification of the radiation interception was easier for a single plant in a bare field, than for a plant located inside a canopy. Indeed, (1) the interaction with the canopy is harder to metamodel, and (2) the aggregated inputs simplify the canopy too much. Simplifying a complex model with many inputs is a principal issue when metamodelling. The complexity of the relationship between inputs is also an issue; for the 3D radiation interception, even small variations in outputs need to be accurately predicted, because small errors amplify over time as a result of the daily retro-acting interactions of light interception and growth. Metamodels based on polynomials are efficient to model all the single variations of the function (Hussain et al., 2002), hence were adapted for the submodel. However, for a general trend, metamodelling based on polynomials cannot provide such a smooth answer. The present study suggests that the polynomial chaos expansion metamodelling, even when performed step by step and improved with expert knowledge, would be inadequate to metamodel the whole FLORSYS model, with its many and diverse inputs. To build a metamodel and estimate sensitivity indices, this method was the most suitable as there is no method that can handle many inputs, metamodelling and estimation of sensitivity indices at the same time.

Consequently, for a global emulation of FLORSYS, in order to synthesize and make available to farmers the knowledge comprised in FLORSYS to help with decision making (Wilkerson et al., 2002), other methods need to be considered. In that case, non-parametric methods can be helpful. Villa-Vialaneix *et al.* (2012) showed that metamodelling methods based on machine learning have good results for medium and large data sets. This is particularly true for Random Forests (Breiman, 2001) which provide the best trade-off between speed and accuracy. Moreover, non-parametric methods can tolerate heterogeneous data sets. This is crucial as FLORSYS with its numerous inputs precludes building a suitable experimental design as the one needed for the present approach.

The global emulation of FLORSYS will be a necessary step to make the model accessible for farmers and crop advisors, particularly for a use in participatory workshops (Colas et al., 2020). Indeed, none

731 of the avenues proposed in Table 6 will be fast enough or compatible with computers used in such as
732 situation.

733 7 Conclusion

734 The present study demonstrated that the frequent practice of developing statistical methods on rather
735 simple case studies makes them difficult and sometimes impossible to apply to more complex real-life
736 situations. Latin Hypercube Sampling (LHS) was used for numerical space filling design, followed by
737 Partial Least Squares regression, combined with a polynomial expansion chaos model and selection of
738 the most influential monomials, to produce simple metamodels. The individual methods used here had
739 trouble handling all the constraints and the domain of validity needed: they (1) eliminated many data
740 close to the limits of the domain of validity of the metamodel (e.g. tiny plants tiny with near-zero leaf
741 areas immediately after emergence) from the simulated data set based on LHS in section 3.1.3,
742 (2) insufficiently accounted for correlations among inputs (e.g. 2-m-tall and 1-cm-narrow plants do not
743 exist) despite using an adapted LHS sampling plan. But both these extreme cases and correlations are
744 frequent in real life and essential for correctly predicting the agroecosystem. Notably, (3) the
745 complexity of radiation transmission and interception inside crop-weed canopies, particularly due to
746 shading by neighbour plants, made it difficult to directly predict radiation absorption at the plant scale.
747 (4) This made it necessary to add functions here, which slowed down simulations again considerably
748 and made us lose most of the speed gain due to the metamodel.

749 So, to simplify a complex process-based weed dynamics model such as FLORSYS, is is essential to
750 combine different methods of sensitivity analysis and model simplification to cover the whole range of
751 relevant stages/morphologies and take account of the complex interactions between plant objects and
752 the many feedbacks during their life cycle. We used a hybrid approach, using a process-based (albeit
753 simplified) approach for the most sensitive plant stage (newly emerged tiny plants) and separate
754 sampling plans and metamodels to ensure that the more sensitive stages/components were adequately
755 covered (small plants). By evaluating the various approaches with independent field observations, we
756 assessed the trade-off between prediction accuracy and simulation speed to identify which modelling
757 approach was best, depending on the objective of the model use.

758 8 Acknowledgements

759 The present work was funded by INRAE (EA and MIA divisions), the French project CoSAC (ANR-
760 14-CE18-0007) and the Burgundy Region. The cropping-system trials were conducted at the INRAE
761 experimental station of Dijon-Époisses, and the weed observations were carried out by Dominique
762 Meunier and colleagues (INRAE Agroécologie Dijon). The paper was greatly improved thanks to the
763 comments of an anonymous reviewer on an earlier version of the manuscript.

9 References

Bagavathiannan, M., Beckie, H., Chantre, G., González-Andújar, J., León, R., Neve, P., Poggio, S., Schutte, B., Somerville, G., Werle, R., Van Acker, R., 2020. Simulation models on the ecology and management of arable weeds: Structure, quantitative insights, and applications. Agronomy 10, 1611.

Berge, T.W., Goldberg, S., Kaspersen, K., Netland, J., 2013. Towards machine vision based site-specific weed management in cereals. Computers and Electronics in Agriculture 81, 79-86.

Bergez, J.E., Colbach, N., Crespo, O., Garcia, F., Jeuffroy, M.H., Justes, E., Loyce, C., Munier-Jolain, N., Sadok, W., 2010. Designing crop management systems by simulation. Eur. J. Agron. 32, 3-9.

Bizouard, G., 2012. Métamodélisation : état de l'art et application., UFR Sciences et techniques. Université de Bourgogne, Dijon, France, p. 60.

Breiman, L., 2001. Random Forests. Machine Learning 45, 5-32.

Breiman, L., Friedman, J.H., Stone, C.J., Olshen, R.A., 1984. Classification and Regression Trees. CRC Press, New York.

Brooks, R.J., Semenov, M.A., Jamieson, P.D., 2001. Simplifying Sirius: sensitivity analysis and development of a meta-model for wheat yield prediction. Eur. J. Agron. 14, 43-60.

Chikowo, R., Faloya, V., Petit, S., Munier-Jolain, N., 2009. Integrated Weed Management systems allow reduced reliance on herbicides and long term weed control. Agriculture, Ecosystems and Environment 132, 237-242.

Cohen, J.B., Prinn, R.G., 2011. Development of a fast, urban chemistry metamodel for inclusion in global models. Atmos. Chem. Phys. 11, 7629-7656.

Colas, F., Cordeau, S., Granger, S., Jeuffroy, M.-H., Pointurier, O., Queyrel, W., Rodriguez, A., Villerd, J., Colbach, N., 2020. Co-development of a decision support system for integrated weed management: contribution from future users. Eur. J. Agron. 114, 126010.

Colbach, N., 2010. Modelling cropping system effects on crop pest dynamics: how to compromise between process analysis and decision aid. Plant Sci. 179, 1-13.

Colbach, N., Bertrand, M., Busset, H., Colas, F., Dugue, F., Farcy, P., Fried, G., Granger, S., Meunier, D., Munier-Jolain, N., Noilhan, C., Strbik, F., Gardarin, A., 2016a. Uncertainty analysis and evaluation of a complex, multi-specific weed dynamics model with diverse and incomplete data sets. Environmental Modelling and Software 86, 184-203.

Colbach, N., Bertrand, M., Busset, H., Colas, F., Dugué, F., Farcy, P., Fried, G., Granger, S., Meunier, D., Munier-Jolain, N.M., Noilhan, C., Strbik, F., Gardarin, A., 2016b. Uncertainty analysis and evaluation of a complex, multi-specific weed dynamics model with diverse and incomplete data sets. Environmental Modelling & Software 86, 184-203.

Colbach, N., Colas, F., Cordeau, S., Maillot, T., Queyrel, W., Villerd, J., Moreau, D., 2021. The FLORSYS crop-weed canopy model, a tool to investigate and promote agroecological weed management. Field Crops Research 261, 108006.

Colbach, N., Colas, F., Pointurier, O., Queyrel, W., Villerd, J., 2017. A methodology for multi-objective cropping system design based on simulations. Application to weed management. European Journal of Agronomy 87, 59-73.

Colbach, N., Collard, A., Guyot, S.H.M., Mézière, D., Munier-Jolain, N.M., 2014. Assessing innovative sowing patterns for integrated weed management with a 3D crop:weed competition model. Eur. J. Agron. 53, 74-89.

Colbach, N., Debaeke, P., 1998. Integrating crop management and crop rotation effects into models of weed population dynamics: a review. Weed Sci. 46, 717-728.

Cox, G.M., Gibbons, J.M., Wood, A.T.A., Craigon, J., Ramsden, S.J., Crout, N.M.J., 2006. Towards the systematic simplification of mechanistic models. Ecological Modelling 198, 240-246.

Debaeke, P., Caussanel, J.P., Kiniry, J.R., Kafiz, B., Mondragon, G., 1997. Modelling crop:weed interactions in wheat with ALMANAC. Weed Research. 37, 325-341.

Deen, W., Cousens, R., Warringa, J., Bastiaans, L., Carberry, P., Rebel, K., Riha, S., Murphy, C., Benjamin, L.R., Cloughley, C., Cussans, J., Forcella, F., Hunt, T., Jamieson, P., Lindquist, J., Wang,

E., 2003. An evaluation of four crop: weed competition models using a common data set. Weed Res. 43, 116-129.
Faivre, R., Iooss, B., Mahévas, S., Makowski, D., Monod, H., 2013. Analyse de sensibilité et exploration de modèles. Editions Quae, Versailles, France 352 pp.
Freckleton, R.P., Stephens, P.A., 2009. Predictive models of weed population dynamics. Weed Res. 49, 225-232.
Gardarin, A., Dürr, C., Colbach, N., 2012. Modeling the dynamics and emergence of a multispecies weed seed bank with species traits. Ecol. Modelling 240, 123-138.
Gauchi, J.P., Bensadoun, A., Colas, F., Colbach, N., 2017. Metamodeling and global sensitivity analysis for computer models with correlated inputs: A practical approach tested with a 3D light interception computer model. Environmental Modelling & Software 92, 40-56.
Gaudio, N., Escobar-Gutierrez, A.J., Casadebaig, P., Evers, J.B., Gérard, F., Louarn, G., Colbach, N., Munz, S., Launay, M., Marrou, H., Barillot, R., Hinsinger, P., Bergez, J.-E., Combes, D., Durand, J.-L., Frak, E., Pagès, L., Pradal, C., Saint-Jean, S., Werf, W.V.D., Justes, E., 2019. Modeling mixed annual crops: current knowledge and future research avenues. A review. Agron. Sustain. Dev. 39, 20.
Graf, B., Gutierrez, A.P., Rakotobe, O., Zahner, P., Delucchi, V., 1990. A simulation model for the dynamics of rice growth and development: Part II-The competition with weeds for nitrogen and light. Agricultural Systems 32, 367-392.
Harrington, P.d.B., Urbas, A., Wan, C., 2000. Evaluation of Neural Network Models with Generalized Sensitivity Analysis. Analytical Chemistry 72, 5004-5013.
Holst, N., Rasmussen, I.A., Bastiaans, L., 2007a. Field weed population dynamics: a review of model approaches and applications. Weed Res. 47, 1-14.
Holst, N., Rasmussen, I.A., Bastiaans, L., 2007b. Field weed population dynamics: a review of model approaches and applications. Weed Res. 47, 1–14.
Hossard, L., Souchere, V., Pelzer, E., Pinochet, X., Jeuffroy, M.H., 2015. Meta-modelling of the impacts of regional cropping system scenarios for phoma stem canker control. Eur. J. Agron. 68, 1-12.
Hussain, M.F., Barton, R.R., Joshi, S.B., 2002. Metamodeling: Radial basis functions, versus polynomials. European Journal of Operational Research 138, 142-154.
Iman, R.L., Conover, W.J., 1982. A distribution-free approach to inducing rank correlation among input variables. Communications in Statistics - Simulation and Computation 11, 311-334.
Kiniry, J.R., Williams, J.R., Gassman, Debaeke, P., 1992. A general, process-oriented model for two competing plant species. Transactions of the ASAE 35, 801-810.
Kleijnen, J.P.C., Sargent, R.G., 2000. A methodology for fitting and validating metamodels in simulation1. European Journal of Operational Research 120, 14-29.
Klem, K., Rajsnerova, P., Novotna, K., Urban, O., Marek, M.V., 2014. Effect of the relative time of emergence on the growth allometry of Galium aparine in competition with Triticum aestivum. Weed Biol. Manag. 14, 262-270.
Kropff, M.J., Spitters, C.J.T., 1992. An ecophysiological model for interspecific competition, applied to the influence of *Chenopodium album* L. on sugar-beet.1. Model description and parameterization. Weed Res. 32, 437-450.
Kropff, M.J., Spitters, C.J.T., Schnieders, B.J., Joenje, W., Degroot, W., 1992. An ecophysiological model for interspecific competition, applied to the influence of *Chenopodium album* L. on sugar-beet. 2. Model evaluation. Weed Res. 32, 451-463.
Lazraq, A., Cléroux, R., Gauchi, J.-P., 2003. Selecting both latent and explanatory variables in the PLS1 regression model. Chemometrics and Intelligent Laboratory Systems 66, 117-126.
Liebman, M., Gallandt, E.R., 1997. Many Little Hammers: Ecological Management of Crop-Weed Interactions, in: Jackson, L.E. (ed.), Ecology in Agriculture. Academic Press, pp. 291-343.
Luo, Z., Wang, E., Bryan, B.A., King, D., Zhao, G., Pan, X., Bende-Michl, U., 2013. Meta-modeling soil organic carbon sequestration potential and its application at regional scale. Ecological Applications 23, 408-420.
Marie, G., Simioni, G., 2014. Extending the use of ecological models without sacrificing details: a generic and parsimonious meta-modelling approach. Methods in Ecology and Evolution 5, 934-943.
Marshall, E.J.P., Brown, V.K., Boatman, N.D., Lutman, P.J.W., Squire, G.R., Ward, L.K., 2003. The role of weeds in supporting biological diversity within crop fields. Weed Res. 43, 77-89.

McKay, M.D., Beckman, R.J., Conover, W.J., 2000. A comparison of three methods for selecting values of input variables in the analysis of output from a computer code. Technometrics 42, 55-61.
Monsi, M., Saeki, T., 1953. Über den Lichtfaktor in den Pflanzengesellschaften und seine Bedeutung für die Stoffproduktion. Japanese Journal of Botany 14, 22-52.
Monsi, M., Saeki, T., 2005. On the factor light in plant communities and its importance for matter production. Annals of Botany 95, 549-567.
Munier-Jolain, N.M., Guyot, S.H.M., Colbach, N., 2013. A 3D model for light interception in heterogeneous crop:weed canopies. Model structure and evaluation. Ecol. Modelling 250, 101-110.
Oerke, E.-C., 2006. Crop losses to pests. Journal of Agricultural Science 144, 31-43
Petit, S., Boursault, A., Le Guilloux, M., Munier-Jolain, N., Reboud, X., 2011. Weeds in agricultural landscapes. A review. Agron. Sustain. Dev. 31, 309-317
Plackett, R.L., Burman, J.P., 1946. The Design of Optimum Multifactorial Experiments. Biometrika 33, 305-325.
Renton, M., 2011. How much detail and accuracy is required in plant growth sub-models to address questions about optimal management strategies in agricultural systems? AoB PLANTS 2011, plr006-plr006.
Renton, M., 2013. Shifting focus from the population to the individual as a way forward in understanding, predicting and managing the complexities of evolution of resistance to pesticides. Pest Management Science 69, 171-175.
Rothenberg, D., Wang, C., 2016. Metamodeling of Droplet Activation for Global Climate Models. Journal of the Atmospheric Sciences 73, 1255-1272.
Saltelli, A., 2002. Making best use of model evaluations to compute sensitivity indices. Computer Physics Communications 145, 280-297.
Stoate, C., Baldi, A., Beja, P., Boatman, N.D., Herzon, I., van Doorn, A., de Snoo, G.R., Rakosy, L., Ramwell, C., 2009. Ecological impacts of early 21st century agricultural change in Europe - A review. Journal of Environmental Management 91, 22-46.
Sudret, B., 2008. Global sensitivity analysis using polynomial chaos expansions. Reliability Engineering & System Safety 93, 964-979.
Tenenhaus, M., 1998. La régression PLS: théorie et pratique. Editions Technip.
Tibshirani, R., 1996. Regression Shrinkage and Selection via the Lasso. Journal of the Royal Statistical Society. Series B (Methodological) 58, 267-288.
Villa-Vialaneix, N., Follador, M., Ratto, M., Leip, A., 2012. A comparison of eight metamodeling techniques for the simulation of N2O fluxes and N leaching from corn crops. Environmental Modelling & Software 34, 51-66.
Waggoner, J., Henneberger, P., Kullman, G., Umbach, D., Kamel, F., Beane Freeman, L., Alavanja, M.R., Sandler, D., Hoppin, J., 2013. Pesticide use and fatal injury among farmers in the Agricultural Health Study. International Archives of Occupational and Environmental Health 86, 177-187.
Wilkerson, G.G., Jones, J.W., Coble, H.D., Gunsolus, J.L., 1990. SOYWEED - a simulation-model of soybean and common cocklebur growth and competition. Agronomy Journal 82, 1003-1010.
Wilkerson, G.G., Wiles, L.J., Bennett, A.C., 2002. Weed management decision models: pitfalls, perceptions, and possibilities of the economic threshold approach. Weed Science Society of America, Lawrence, KS, ETATS-UNIS 14 pp.
Wold, S., Sjöström, M., Eriksson, L., 2001. PLS-regression: a basic tool of chemometrics. Chemometrics and Intelligent Laboratory Systems 58, 109-130.

10 Illustrations

Table 1: Compilation of different sensitivity analysis methods for independent variables depending on complex model's proprieties. From (Tenenhaus, 1998; Harrington et al., 2000; Bizouard, 2012; Faivre et al., 2013; Gauchi et al., 2017)

	ANOVA	Sobol-Saltelli	FAST	PCE-OLS	PCE-PLS	CART; random forest	Neural network
Model characteristics							
Inputs number > 10	difficult to test all interactions	Yes	difficult, too heavy	Yes	Yes	Yes	Yes
Possible run number > 1000	Yes	Yes	Yes	Yes	Yes	Yes	Yes
Accepts correlated inputs	No	No	No	No	Yes	Yes	Yes
Properties of sensitivity methods							
Estimates sensitivity indices	Yes	Yes	Yes	Yes	Yes	No	No
Evaluates inputs for their importance	Yes	Yes	Yes	Yes	Yes	Yes	Yes
Provides a metamodel	Yes	No	No	Yes	Yes	Yes	Yes
Simulation design available from: LHS, Sobol sequence, Monte-Carlo, Hadamard, Full factorial design, Morris, OAT, numerous data from different sources	all	LHS, Sobol sequence, Monte-Carlo	Monte-Carlo	LHS, Sobol sequence, Monte-Carlo	LHS, Sobol sequence, Monte-Carlo	all	all

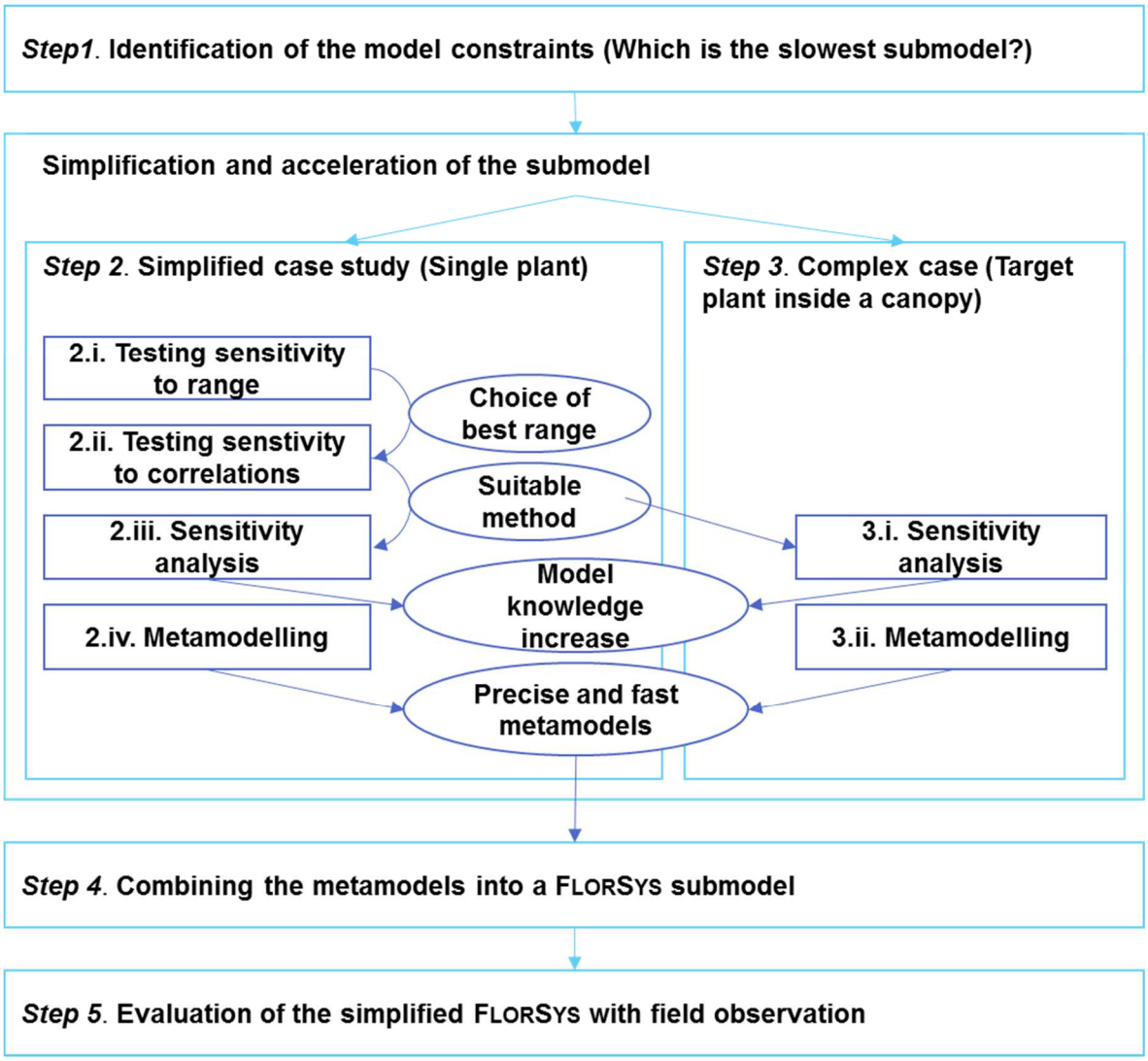

Figure 1: Schematic representation of the steps of the simplification and acceleration of the model FLORSYS. The Arabic numbers and roman numbers correspond to, respectively, the sections and sub-sections of the paper (Floriane Colas © 2017).

928 Table 2: Definition, range variation and unit of the inputs and outputs of the 3D radiation interception
929 submodel.
930 A. Inputs

Type	Name	Short explanation	Step[§]	Range of variation	Unit
Physical environment	Latitude	Latitude of the simulated field	both	[-66; +66] single plan [0; +66] plant in a canopy	angle degree
	Day	Julian day	both	[1; 365]	no unit
Model precision	Xmax	Field sample size in the East-West direction	SP	[1; 4]	m
	Ymax	Field sample size in the North- South direction	SP	[1; 4]	m
	Voxel	Voxel edge size	SP	[1; 20]	cm
Target-plant variables	Height	Plant height	both	[1; 250]	cm
	Width	Plant width	both	[1; 200]	cm
	LA	Total plant leaf area	both	[1; 10^5]	cm2
	k	Species radiation extinction coefficient	both	[0.01; 1.1]	no unit
	RH50	Relative median leaf height below which is located half of the leaf area	both	[0.01; 1]	$cm \cdot cm^{-1}$
	b	Shape parameter for leaf distribution vs. plant height	both	[0.01; 6]	no unit
Neighbour mean plant variables	Density	Total plant density of the disc of plants (crops + weeds), including the target plant	PIC	[0.1; 3000]	$plant.m^{-2}$
	Distance to neighbour	Distance of the target plant to the furthest neighbour	PIC	[0.1; 3]	m
	Height	Plant height averaged over all neighbours and weighted by the inverse of distance to target plant	PIC	[0; 240]	cm
	Cover	Plant base area (superposed plants are added to the value) averaged over all neighbours and weighted by the inverse of distance to target plant	PIC	[0; 20000]	cm^2
	LA	Plant leaf area averaged over all neighbours and weighted by the inverse of distance to target plant	PIC	[0; 100000]	cm^2
	k	Species extinction coefficient averaged over all neighbours and weighted by the inverse of distance to target plant	PIC	[0; 0.7]	no unit
	RH50	Plants relative height averaged over all neighbours and weighted by the inverse of distance to target plant	PIC	[0; 115]	cm

931 [§] Input used in the "Single Plant" step (SP), the "Plant Inside a Canopy" step (PIC) or both
932

B. Outputs (for target plant)

Use for FLORSYS	Name	Short explanation	Step[§]	Range of variation	Unit
Growth submodel	PARaP	Proportion of PAR[&] absorbed by the plant at the plant scale compared to the PAR above canopy.	both	[0; 1]	MJ cm^{-2} MJ^{-1} cm^2 $plant^{-1}$
	PARaC	Proportion of PAR absorbed by the plant for 1 cm^3 compared to the PAR above canopy	both	[0; 1]	MJ cm^{-2} MJ^{-1} cm^2 cm^{-3}
Morphology submodel	SID	Daily Shading Intensity , *i.e.* proportion of incident radiation above canopy that does not reach the plant	both	[0; 1]	MJ MJ^{-1}
Herbicide treatment submodel	$rPARi_{plant}$	Proportion of radiation intercepted by the plant relative to incident radiation above canopy	both	[0; 1]	MJ.cm^{-2} MJ^{-1} cm^2
	$rPARi_{top}$	Proportion of radiation intercepted by the top of the plant relative to incident radiation above canopy	PIC	[0; 1]	MJ.cm^{-2} MJ^{-1} cm^2
	$rPARi_{base}$	Proportion of radiation intercepted by the base of the plant relative incident radiation above canopy	both	[0; 1]	MJ.cm^{-2} MJ^{-1} cm^2

[&] PAR: Photosynthetically Active Radiation; [§] Output computed for the "Single Plant" step (SP), the "Plant Inside a Canopy" step (PIC) or both

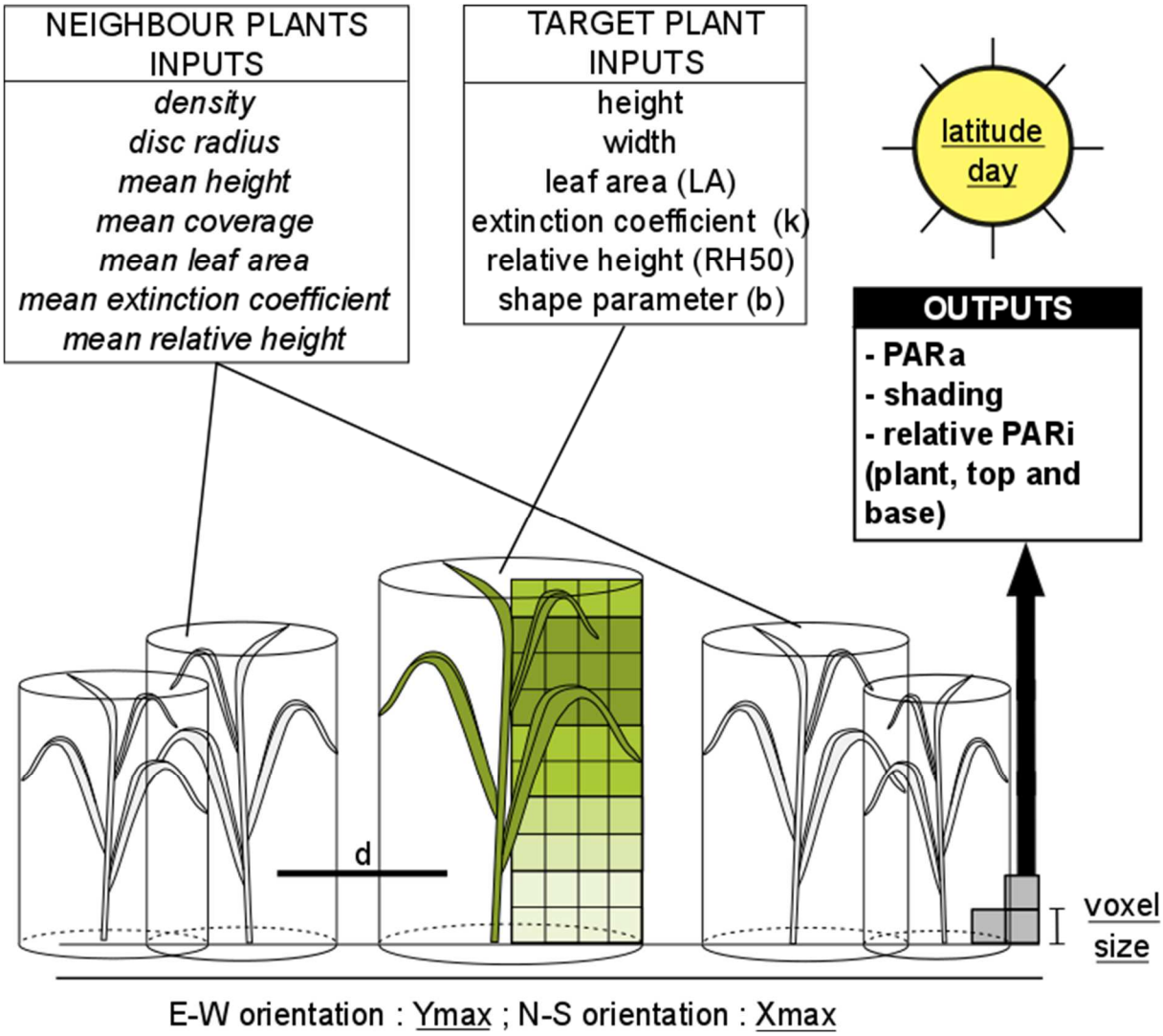

Figure 2: Schematic representation of the inputs and outputs of the 3D radiation interception submodel of FLORSYS (MUNIER-JOLAIN ET AL., 2013), with environmental and precision inputs (underlined), *plant in a canopy inputs (italics)*, single plant common inputs (standard font) and outputs (bold). For abbre*via*tions, see Table 2. (Floriane Colas © 2017 updated from (Gauchi et al., 2017))

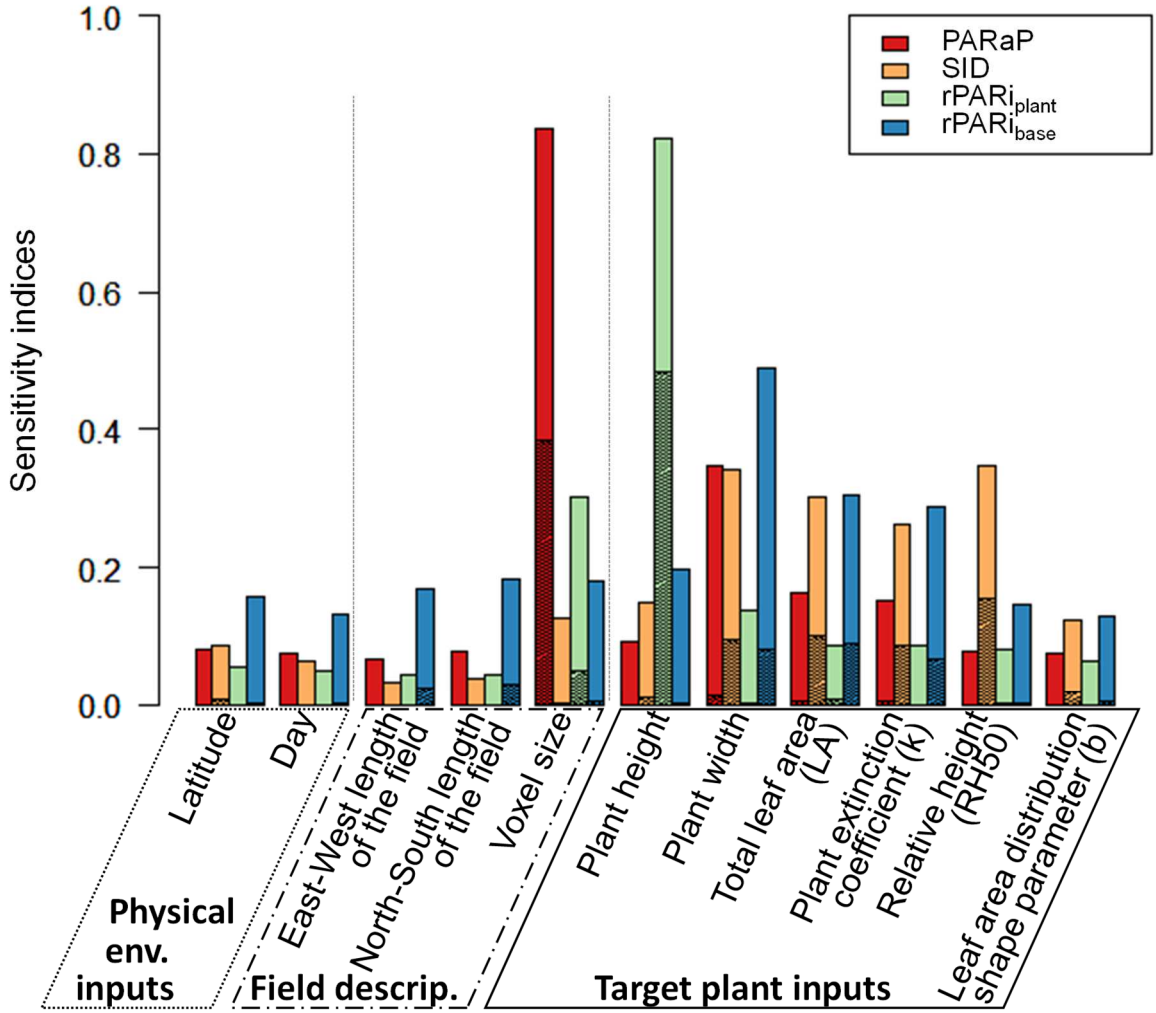

944

945 Figure 3 : Overall view of sensitivity indices for radiation interception outputs of a target plant, in the
946 absence of any shading neighbour plants. In hatched colours polynomial effects (*i.e.* disregarding
947 interactions), in plain colours total effect (including interactions) of the inputs, environmental and
948 precision inputs (underlined) and single plant input (normal font). The outputs are the Photosynthetic
949 Active Radiation (PAR) absorbed by the target plant (PARaP), shading index (SID), relative PAR
950 intercepted by the whole plant ($rPARi_{plant}$) or on soil surface ($rPARi_{base}$). (Floriane Colas © 2018)

951

952

Table 3: Synthesis of the different 3D radiation interception metamodels (fast and full) computed *via* polynomial chaos expansion (PCE) and Partial Least Squares (PLS) regression. Fast metamodels result from full metamodels via a LASSO-PLS monomials selection.

A. Single target plant without shading neighbouring plants

	Radiation-interception model output	Metamodel type	Polynomial degree	Monomial number	Fitting prediction Q2cum	Prediction error RMSEP[§]
[1]	PARaC	full	5	4367	0.96	0.19
[2]	PARaC	fast	5	26	0.85	0.39
[3]	SID	full	5	4367	0.98	0.15
[4]	SID	fast	5	26	0.82	0.43
[5]	$rPARi_{plant}$	full	5	4367	0.95	0.22
[6]	$rPARi_{plant}$	fast	5	27	0.90	0.32
[7]	$rPARi_{base}$	full	5	4367	0.93	0.25
[8]	$rPARi_{base}$	fast	5	25	0.70	0.55

B. Target plant inside a canopy

	Radiation-interception model output	Metamodel type	Polynomial degree	Monomial number	Fitting prediction Q2cum	Prediction error RMSEP[§]
[9]	PARaC	full	4	3875	0.83	0.33
[10]	PARaC	fast	5	30	0.56	0.65
[11]	SID	full	4	3875	0.75	0.42
[12]	SID	fast	5	29	0.30	0.83
[13]	$rPARi_{top}$	full	4	3875	0.71	0.48
[14]	$rPARi_{top}$	fast	5	28	0.27	0.85
[15]	$rPARi_{plant}$	full	7	4000	0.82	0.36
[16]	$rPARi_{plant}$	fast	5	35	0.52	0.69
[17]	$rPARi_{base}$	full	4	3875	0.76	0.43
[18]	$rPARi_{base}$	fast	5	35	0.37	0.79

[§] root mean squared error predictor

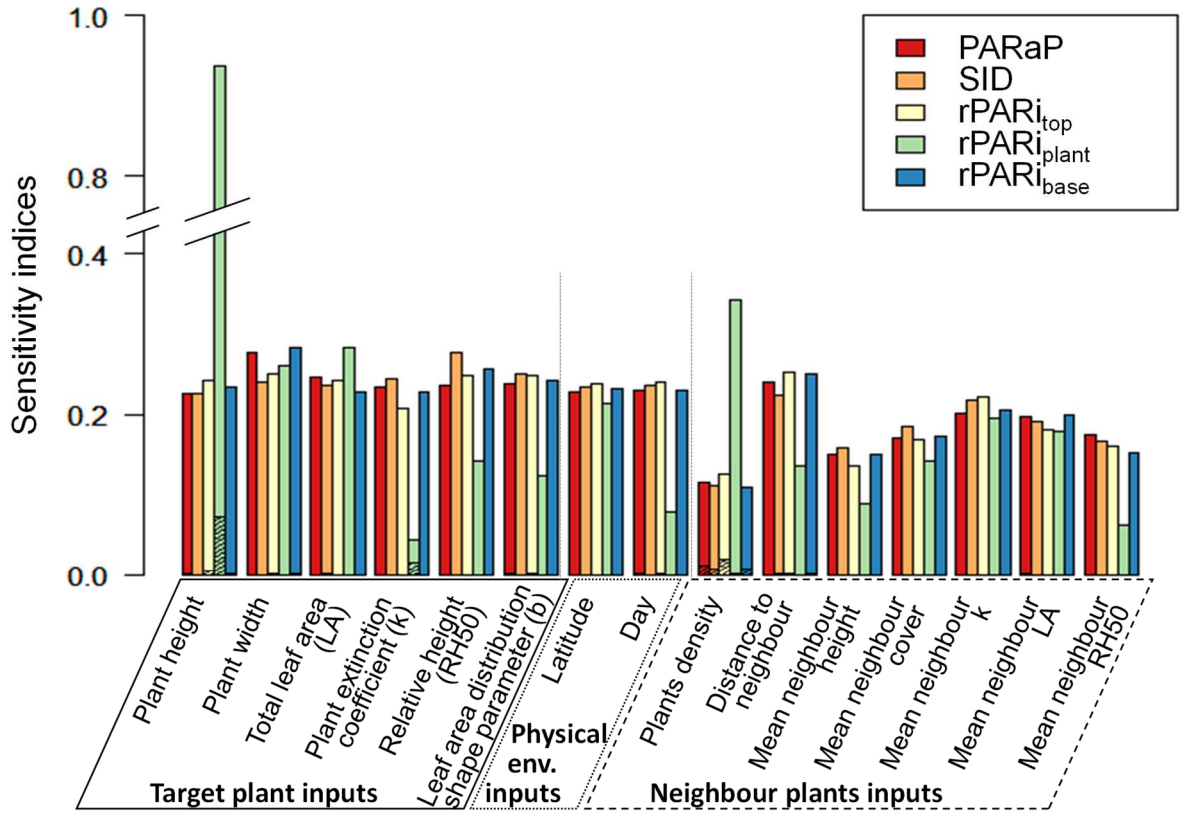

961

962 Figure 4: Overall view of sensitivity indices for radiation interception outputs of a target plant
963 surrounded by neighbour plants. Total effects (plain colours) and polynomial effects (*i.e.* disregarding
964 interactions, hatched colours) of inputs of the FLORSYS radiation interception submodel. The outputs
965 are the Photosynthetic Active Radiation (PAR) absorbed by the target plant (PARaP), shading index
966 (SID), relative PAR intercepted at the summit of the target plant ($rPARi_{top}$), by the whole plant
967 ($rPARi_{plant}$) or at the base of the target plant ($rPARi_{base}$). (Floriane Colas © 2017)

968

969

970 Table 4 : Synthesis of the variation in prediction error in simulations with the metamodelled *vs.*
971 process-based model. Relative root mean squared error predictor (RRMSEP) in relation to variation
972 range of observation (max-min)/2.

Output	Species scale	Time step	Type of neighbours used for calculating canopy variables		
			Local	Mixed	Average
Weed density (plants·m^{-2})	By species	Day	+9%	++%$^{\$}$	+10%
		Multiannual	-81%	-7%	-52%
	Sum of all species	Day	+9%	++%$^{\$}$	-85%
		Multiannual	-50%	-8%	+152%
Weed biomass (g·m^{-2})	By species	Day	+294%	+417%	+580%
		Multiannual	++%$^{\$}$ for process-based model		
	Sum of all species	Day	++%$^{\$}$.	+327%	+723%
		Multiannual	+1351%	+10353%	+12391%
Seedbank (seeds·m^{-2})	By species	Day	+164%	+163%	+84%
	Sum of all species	Day	++%$^{\$}$ for process-based model		
Crop yield (T·ha^{-1})	By species	Day	+61%	+6%	79%

973 $^{\$}$ RRMSEP of metamodelled simulation was >> 0 and RRMSEP of process-based simulation was <
974 variability in observations, *i.e.* ~0, and no relative variation in RRMSEP could be calculated

975

976

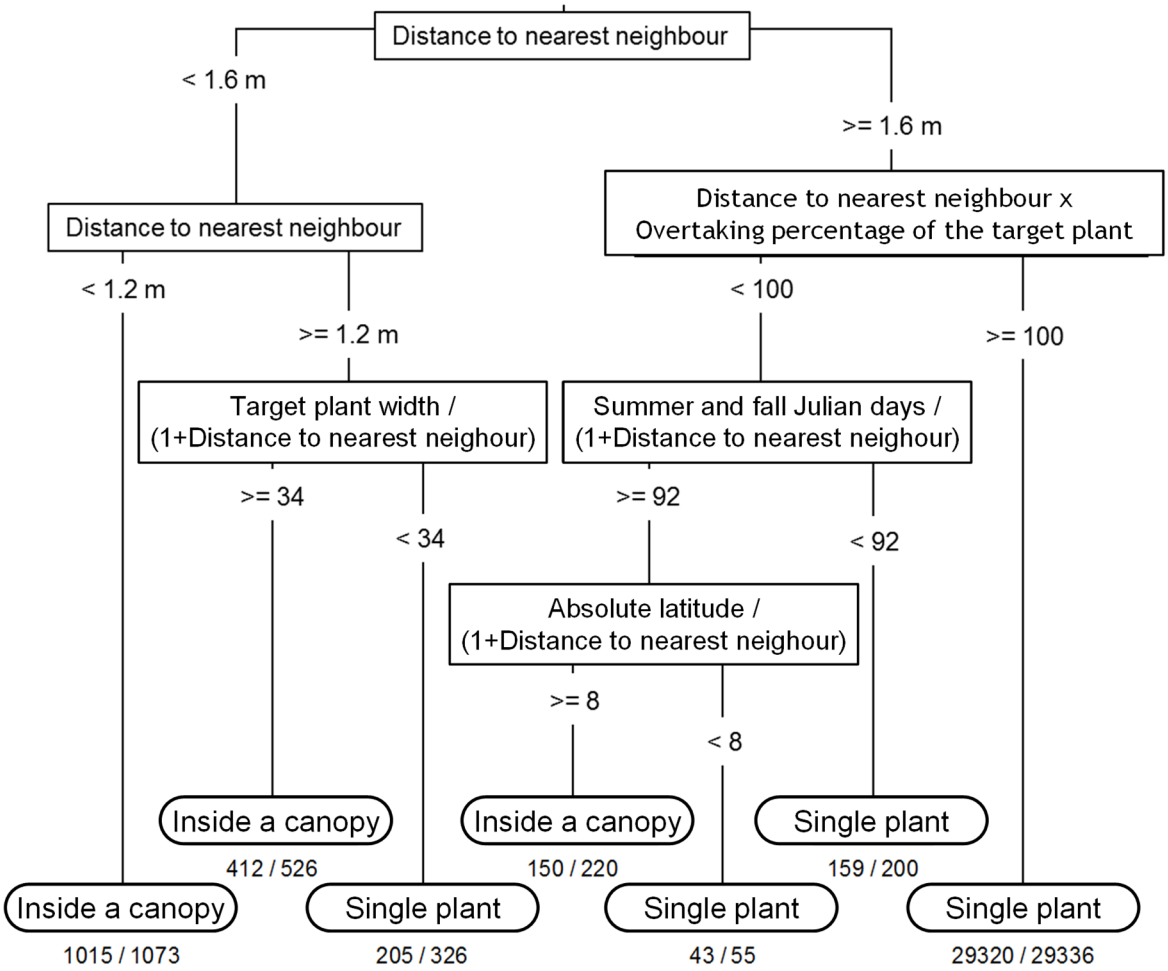

977

978 Figure 5: Classification tree (CART) to decide whether a target plant is single or inside a canopy. The
979 segmentation is based on relative photosynthetically active radiation on target-plant top $rPARi_{top}$>
980 0.98. The adjustment error (or training error) was 0.24, the cross validation error was 0.28 (standard
981 deviation = 0.01). (Floriane Colas © 2017)

982

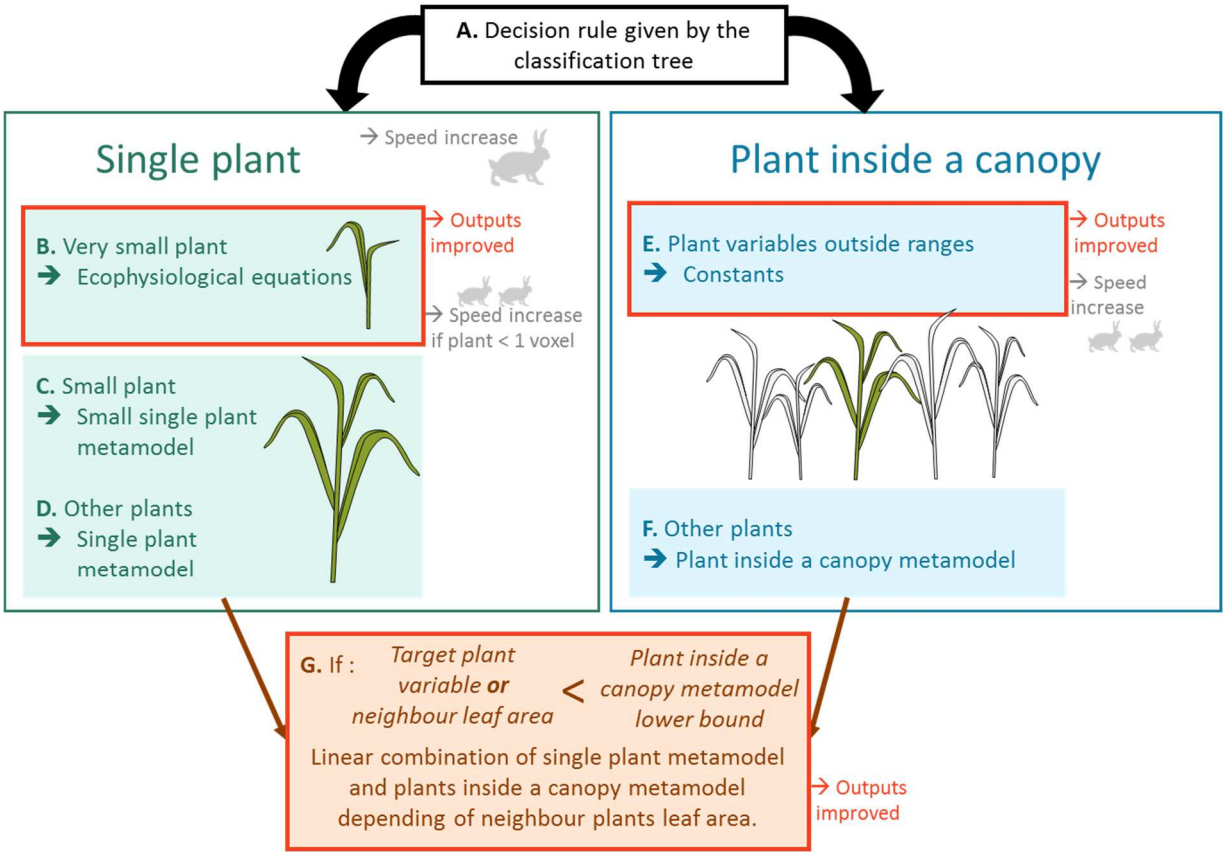

983

984 Figure 6: The different metamodels and when they are used in FLORSYS-ML depending on target plant
985 variables, neighbour plant variables and environmental variables. (Floriane Colas © 2017)

986

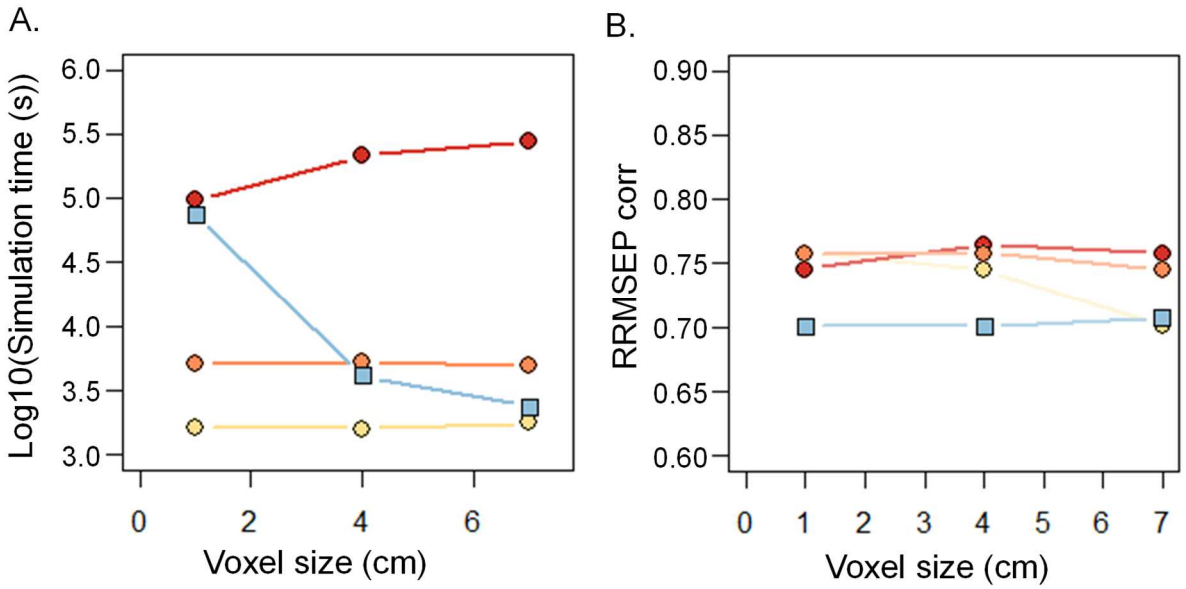

Figure 7: Simulation time (A) and prediction error (relative root mean squared error predictor RRMSEP, B) of the daily weed seedbank by species for the different FLORSYS versions (squares: process-based, circles: metamodelled FLORSYS-ML), neighbour-aggregrating methods (dark red: local neighbours, light yellow: average, orange: mixed) and voxel edge sizes. Relative error in relation to variation range of observation (max-min)/2 (Floriane Colas © 2017)

995 Table 5 : Synthesis table to guide the choice of the best simulation method with the smaller prediction error (relative root mean squared error predictor
996 RRMSEP) depending on the goal and the target output.

Output	Species scale	Time step	Simulation goal	
			Farmer's workshops (fast simulations: 7 cm voxel, 6x3 m² field)	Site-specific weed management (precise simulations : 1 cm voxel, 6x3 m² field)
Weed density (plants·m^{-2})	By species	Day	Process-based	Process-based #
		Multiannual	Metamodelled with average neighbours	Metamodelled with average neighbours *
	Sum	Day	Process-based	Process-based #
		Multiannual	Process-based	Process-based
Weed biomass (g·m^{-2})	By species	Day	Process-based	Metamodelled with local + average &
		Multiannual	Metamodelled with local neighbours	Metamodelled with local + average neighbours
	Sum	Day	Process-based	Metamodelled with local + average &
		Multiannual	Metamodelled with local neighbours	Metamodelled with local + average neighbours
Seedbank (seeds·m^{-2})	By species	Day	Process-based *	Process-based
	Sum	Day	Metamodelled with local + average &	Metamodelled with local neighbours
Crop yield (T·ha^{-1})	By species	Day	Process-based	Process-based

997 Other methods that are also close in the RRMSEP value: * all of the other methods; & metamodel with average neighbour; # metamodel with local neighbours

998

999

1000 Table 6 : Summary of avenues for speeding up complex models such as FLORSYS

Method		Advantage	Disadvantage	Best use for…
Model modification				
1	Simpler light interception models	Simpler process-based	Cannot represent heterogeneous crop canopies	Homogeneous (single-species) canopies, uniform field management
2	Metamodel	Simpler light interception, identification of key factors for light interception	Lose connection of processes, cannot wholly grasp the complexity of plant-plant interactions	Precision agriculture, very heterogeneous multispecies canopies,
Input choice				
3	Increase voxel size, decrease field-sample area	No source modification needed	Precision loss	Canopies with little heterogeneity and few species, uniform field management
Technical solutions				
4	Parallel source processing, graphical processing units	Remain process-based	Not "portable" to all computers	Research, all cropping systems
5	Powerful computers, calculation servers	No source modification needed	Not accessible to non-researchers	Research, all cropping systems

1001

1002